

Adsorption of anionic azo dye from aqueous wastewater using zeolite NaX as an efficient adsorbents

Rasha H. Khudhur^a, Nisreen S. Ali^b, Eman H. Khader^a, Noor S. Abbood^a, Issam K. Salih^c, Talib M. Albayati^{a,*}

^aDepartment of Chemical Engineering, University of Technology-Iraq, 52 Alsinaa St., P.O. Box: 35010, Baghdad, Iraq, emails: Talib.M.Naieff@uotechnology.edu.iq (T.M. Albayati), Rasha.H.Khudhur@uotechnology.edu.iq (R.H. Khudhur), noor.s.abbood@uotechnology.edu.iq (N.S. Ali), eman.h.khader@uotechnology.edu.iq (E.H. Khader)

^bMaterials Engineering Department, College of Engineering, Mustansiriyah University, Baghdad, Iraq, email: nisreensabah@uomustansiriyah.edu.iq

^cDepartment of Chemical Engineering and Petroleum Industries, Al-Mustaqbal University, Babylon 51001, Iraq, email: dr_issamkamil@mustaqbal-college.edu.iq

Received 20 January 2023; Accepted 18 August 2023

ABSTRACT

In this investigation, batch adsorption was utilized to get rid of the anionic azo dye from an aqueous solution. Adsorbents based on zeolite NaX were used. The results showed that zeolite NaX adsorbents achieved greater removal efficiency with values of 72.34%. According to the findings, with $R^2 = 0.9958$, adsorption model using the Langmuir isotherm showed a greater correlation coefficient. When the Freundlich, Temkin, and Langmuir isotherm adsorption models were assessed. According to type Langmuir isotherm adsorption, 0.42187 mg/g was established as the maximal absorption of azo dye. The Langmuir isotherm model's equilibrium parameter (R_L) values showed that all R_L values were between 0 and 1, demonstrating the favorability of the Langmuir isotherm. Pseudo-first-order and pseudo-second-order models were used to examine adsorption kinetics. It was discovered that the pseudo-first-order kinetics of the zeolite NaX adsorption rates were supported, with R^2 values of 0.9894 for the high connection. The outcomes demonstrated zeolite NaX's moderate dye removal efficiency.

Keywords: Zeolite NaX; Azo dye; Adsorption; Wastewater treatment; Batch adsorption; Adsorption kinetics; Water pollution; Water remediation; Isotherms

1. Introduction

The textile sector is now recognized as a substantial and serious cause of water quality issues by discharging large volumes of effluent into surface water bodies since it creates large volumes of highly contaminated wastewater [1,2]. Considering its chemical makeup, which consists of organic compounds, colors, and detergents, this type of wastewater is also seen as dangerous and highly polluted [3,4]. The widespread use of organic dyes in the paper, textile, and apparel industries has resulted in severe environmental

contamination [5,6]. Common organic pollutants identified in aquatic habitats include dyes, drugs, surfactants, phenols, and pesticides [7,8]. Numerous environmental issues arise as a result of the discharge of this highly polluted effluent into aquatic environments. For example, it produces unpleasant colors and smells [9], inhibits sunlight penetration, which is bad for aquatic life [9,10], and lowers the concentration of dissolved oxygen [11]. Azo-dye is regarded as dangerous to humans because to the possibility of it causing thyroid cancer, eczema, migraines, blurred vision, itching, hyperactivity, and other medical

* Corresponding author.

and behavioural problems [12]. Contrarily, azo dyes may degrade into long-lasting hazardous byproducts after they are received [13]. Membrane separation, anaerobic or aerobic treatment, coagulation, electrochemical oxidation, chemical oxidation, microbial degradation, filtering, and chemical oxidation are some of the (chemical, physical, and biological) methods used to get rid of this colour [14–17]. The drawbacks of some of these methods include significant expenses, the creation of secondary pollutants, and labour-intensive, unsuccessful processes, and low removal rates [18]. Adsorption has been utilized more frequently than other approaches to remove synthetic colors from aqueous effluents due to its ease of use, capacity to regenerate the adsorbents, immunity to hazardous compounds, low cost, and treatment efficacy even with diluted solution [19–23]. Additionally, it does not produce sludge, in contrast to chemical precipitation or coagulation–flocculation processes [24]. Zeolite NaX was first used in many of chemical industries as ion exchangers, adsorbents, or catalysts to remove organic pollutants such colors from industrial effluent [25]. An indisputable advantage of zeolites is their low influence on aging, especially when exposed to radiation [26]. The adsorbents must also be sufficient for removing different types of color.

This study looked at the efficiency of zeolite NaX as a commercial adsorbent for batch-level azo dye adsorption from industrial wastewater. The pH, contact time, dye concentrations, and adsorbent dose were some of the variables we examined. Isotherm and kinetic experiments were also performed to evaluate the dye removal process' efficacy and the adsorbents' capacity. The theoretical framework provided by this study can be used to increase the efficacy of commercial materials as adsorbents in the reduction of anionic dye pollution.

2. Materials and methods

2.1. Chemicals

Anionic dye, also known as E102, FD&C Yellow 5, or Acid Yellow 23, was provided by the Sigma-Aldrich Company of Germany and has a molecular weight of 534.4. 426 nm is the wavelength of it. A stock dye solution was created using the dye (0.5 g) and water, each liter of distilled water contains 0.5 g of color. The resulting mixture was adjusted to obtain the test starting concentrations after being compared to industrial effluent concentrations at the Main Corporation of the Textile Iraqi Sector. pH values were then controlled using 97% and 98% pure NaOH and HCl, respectively, obtained from Sigma-Aldrich Company (Germany). Zeolite NaX (purity 99.9%) was acquired from Central Drug House in Iran.

2.2. Preparation and properties of adsorbent

In this work, 1.3 mm-diameter zeolite NaX [Na₈₁(AlO₂)₈₁(SiO₂)₁₁₁] with a bulk density of 650 g/L was used. Prior to use, zeolite NaX was cleaned with water, treated with a 1 M MgCl₂ solution, and dried at 373 K. The pH of the mixture was thereafter changed continuously using solutions of sodium hydroxide and hydrochloric acid. Furthermore, laboratory-grade chemicals were employed

for experimentation, whereas analytical-grade chemicals were used for analysis. Throughout the entire investigation, deionized water was used.

2.3. Batch adsorption experimental setup

In this investigation, batch adsorption experiments were carried out to determine the ideal conditions for azo dye removal at an ambient temperature of 23°C, a variety of adsorbents, a pH range of 2 to 10, 0.1–0.5 g of adsorbent, and other ingredients. 5–45 mg/L of dye was present in the samples. 50 mL of the measurement solution was then added to 100 mL beaker with a predetermined amount of synthetic material at its starting concentration of dye and pH. A mechanical shaker (the German-made Heidolph Unimax 1010 Model, which continually shook at 150 rpm) was used to shake the test solution until the pH values were as required using either 1 M NaOH or 1 M HCl. After the interval duration was established, samples were taken and centrifuged for 10 min to distinguish the adsorbent from the mixture at 2,500 rpm. A double-beam spectrophotometer and spectrophotometric equipment (Jenway 6850, Germany) were used to measure the amount of dye still present in the supernatant at 426 nm. The percentage of dye elimination was calculated using the following equation:

$$\text{Percentage of dye removal} = \frac{(C_0 - C_e)}{C_0} \times 100\% \quad (1)$$

where C_0 (mg/L) is the starting concentration of dye and C_e (mg/L) the equilibrium concentration.

2.4. Isotherms adsorption

Isotherm adsorption determines the state of equilibrium between the sorbate and the adsorbent. the ratio of the amount remained in the solution to that which has been adsorbed at equilibrium and constant temperature. To select the most appropriate model to be used throughout the design phase, data on isotherm must be proportioned appropriately with different isotherm models [27]. In this work, Langmuir, Freundlich, and Temkin's three isotherm models were investigated. Eq. (2) represents the Langmuir model equation:

$$\frac{C_e}{q_e} = \frac{1}{bq_{\max}} + \frac{C_e}{q_{\max}} \quad (2)$$

where C_e (mg/L) is the azo dye concentration, q_e (mg/g) equilibrium adsorption capacity, and b (L/mg) the equilibrium's Langmuir constant. It is possible to calculate the maximum capacity of adsorption (q_{\max} (mg/g)), employing a (C_e/q_e) vs. C_e plot and its slope and intercept. Such a formula suggests that an azo dye monolayer was applied to the face of the adsorbent surface of the zeolite NaX, which has been used successfully in several adsorption processes. The separation factor known as dimensionless equilibrium constant (R_L) has the following form [28,29]:

$$R_L = \frac{1}{1 + bC_0} \quad (3)$$

The value of R_L indicates four possible conditions of the isotherm: (1) favorable ($R_L < 1$), (2) unfavorable ($R_L > 1$), (3) linear ($R_L = 1$), or (4) irreversible ($R_L = 0$) [30].

Furthermore, at constant energy, heterogeneous surfaces serve as the foundation for the Freundlich isotherm and does not impose any restrictions on the formation of monolayers. A heterogeneous system is defined by the Freundlich isotherm, an empirical equation. The linearized Freundlich isotherm's equation is:

$$\ln q_e = \frac{1}{n} \ln C_e + \ln k_f \tag{4}$$

where k_f and $1/n$ are the adsorption capacity at a given concentration and the adsorption intensity, respectively.

One of the characteristics of the Temkin isotherm model that is well displayed is the relationship that exists between the particle that is being absorbed and the adsorbent. The models presented below as Eq. (5) were developed using this model:

$$q_e = B \ln C_e + B \ln A \tag{5}$$

$$B = \frac{RT}{b} \tag{6}$$

The constants A and B , which are comparable to the Temkin constants for the heat of adsorption (b) (J/mol) and the gas constant R (8.314 mol/K), respectively, were calculated by plotting q_e vs. $\ln C_e$. B is a Temkin isotherm constant equivalent, while T is the absolute temperature in K. By considering the adsorption, a Temkin graph of the q_e vs. $\ln C_e$ is produced. using a spectrophotometer and the previously indicated connection, as well as its derived parameters [31].

2.5. Adsorption kinetics models

The adsorption rate constant can be calculated using the pseudo-first-order Eq. (7) [32]:

$$\ln(q_e - q_t) = \ln q_e - k_1 t \tag{7}$$

where q_e and q_t (mg/g) are the amounts of azo dye adsorbed at equilibrium and t is time (min), k_1 (min) is the pseudo-first-order adsorption rate constant.

Another sort of kinetic model that clarifies the kinetics of the adsorption process is pseudo-second-order [33]. The form of this kinetic equation is as follows:

$$\frac{t}{q_t} = \frac{1}{k_2 q_e^2} + \frac{t}{q_e} \tag{8}$$

where (q_e) is the equilibrium adsorption capacity and k_2 (g/mg·min) is the second-order constant, respectively.

The intraparticle diffusion model is in Eq. (9) [34]:

$$q_t = k_{id} t^{0.5} + C \tag{9}$$

where k_{id} (mg/g·min^{0.5}) indicates the constant for the intraparticle diffusion rate, while C indicates the constant related

to intraparticle diffusion. If a line can be drawn when plotting q_t vs. $t^{0.5}$, it signifies that the adsorption process is limited to intraparticle mass transfer. But if a number of linear plots can be drawn using the same data, it demonstrates that the adsorption process has been greatly influenced by the multiple phases associated with the aforementioned stages. The values of C indicate the boundary layer thickness, with a lower values of the intercept signifying that the boundary layer has less of an effect [35].

3. Results and discussions

3.1. Batch adsorption

The effects of numerous variables, including contact time (10–140 min), pH (2–10) beginning concentration of azo dye (5–45 mg/L), and the speed of shaking (100–180 rpm), were studied using dosages of zeolite NaX adsorbents (0.1–0.5 g).

3.1.1. Effect of contact time

Fig. 1 shows how changing the contact duration from 10–120 min has an effect on the percentage of dye removal at 5 mg/L. The percentage removal increased as contact duration increased and eventually stabilized. This could be the result of zeolite NaX reaching equilibrium. As demonstrated, initially rising then falling over time, the rate of azo dye adsorption. In contrast to the latter, slower rate of azo dye adsorption, the surface of the adsorbent had less active sites than was required early on [36]. Similar trends for dye removal [37] and organic acid removal [38] from a variety of adsorbents have been documented in the literature. Adsorption of the dye and adsorbents achieved equilibrium after 120 min of contact time. The removal efficiency for an azo dye concentration of 5 mg/L using zeolite NaX was 57.75%.

3.1.2. pH effects

The pH is one of the most crucial factors in the procedure of adsorption since it can affect the properties of the

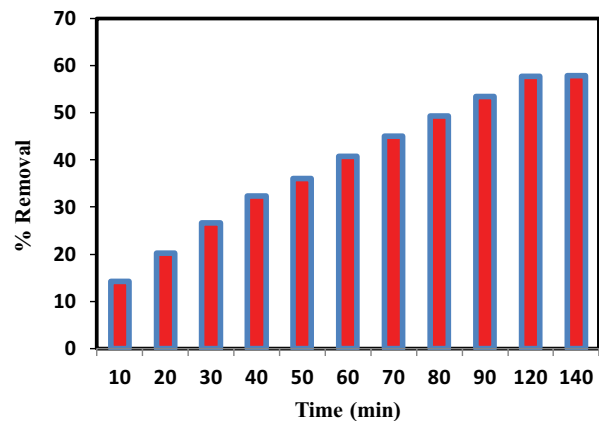


Fig. 1. Effect of contact time on adsorption of azo-dye at azo dye concentrations = 5 mg/L, pH = 5, temperature = 23°C, zeolite NaX adsorbents dose = 0.3 g, and shaking rotary speed = 200 rpm.

metal in solution and the load of the active sites on the surface [39]. In this study, the impact of pH on the adsorption of the azo dye adsorption was examined. The pH range for the azo dye adsorption experiments was 2–10, and the temperature was 23°C. According to Fig. 2, pH 2 had the highest removal efficiency when it came to dye adsorption by zeolite NaX, whereas pH 10 had the lowest. The existence of anionic azo dye in decomposed shape as dye ions in aquatic fluids can be utilized to explain this. Anionic azo dye includes an intense electrostatic draw to the positively charged objects of zeolite NaX at low pH levels, boosting dye absorption. Adsorbent surfaces become negatively charged and the positive charge sites on them contract at high pH values. In this case, there was some electrostatic repulsion, which caused some azo to be absorbed from the water solution [40,41]. Additionally, OH⁻ ions successfully compete with dye ions when pH rises to lessen dye adsorption. Studies utilizing corn silage to study dye adsorption have found that when pH increases, dye adsorption efficiency decreases [42]. Zeolite NaX indicated clearance rates of 66.97% at 0.2 g/100 mL dye after 120 min at lower pH values.

3.1.3. Effect of adsorbent dosage

Fig. 3 depicts how the adsorbent dosage affected the elimination of azo dye until 0.3 g, the percentage of azo dye removal rises before falling. As adsorbent dose rises, less dye is absorbed per unit of adsorbent weight, lowering the adsorption capacity (mg/g). Adsorption capacity is reduced in this situation as a result of high adsorbent concentration and increased accessibility to active sites. As a result, dye removal is constrained when adsorbent concentration is rising while dye concentration is steady [43]. As a result, zeolite NaX adsorbents (0.3 g) was decided upon as the ideal dosage. After 120 min and 5 mg/L concentration of azo dye, zeolite NaX (0.3 g) had a 68.32% removal efficiency of azo dye.

3.1.4. Impact of azo dye's initial concentration

When zeolite NaX 0.3 g/100 mL is used as an adsorbent, The effectiveness of the removal is shown in Fig. 4 in

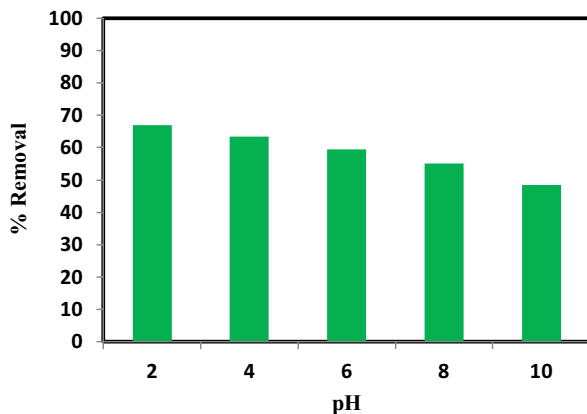


Fig. 2. Effect of pH on adsorption of azo-dye at contact time = 120 min, azo dye concentrations = 5 mg/L, temperature = 23°C, zeolite NaX adsorbents dose = 0.3 g, and shaking rotary speed = 200 rpm.

relation to the range 5–45 mg/L of azo dye concentration. In the tests, 23°C, pH 2, and 120 min contact time were all used. As the original azo dye concentration grew, it appeared that the efficacy of azo dye removal dropped, as illustrated in Fig. 4. The adsorbent layer was found to be saturated at spots of adsorption [44]. Which was based on the hypothesis of monolayer dye most likely developed at the interface of adsorbent dye. The increase in azo dye starting concentration facilitates additional interactions between azo dye molecules and adsorbents. Thus, the pushing power of the concentration gradient increases [45]. Zeolite NaX enabled the elimination of the azo dye 68.32% at a concentration of 5 mg/L, compared to 46.56% at a concentration of 45 mg/L.

3.1.5. Shaking speed effects

By adjusting the speed of shaking from 100 to 180 rpm, it was feasible to assess how the elimination of azo dye by

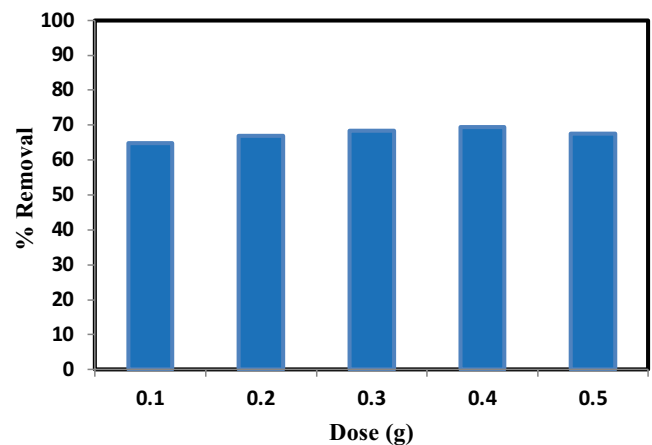


Fig. 3. Effect of zeolite NaX adsorbent dose on adsorption of azo-dye at contact time = 120 min, azo dye concentrations = 5 mg/L, pH = 2, temperature = 23°C, and shaking rotary speed = 200 rpm.

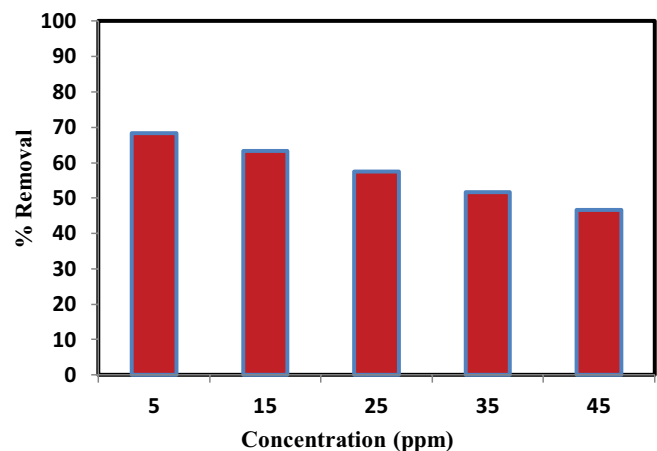


Fig. 4. Effect of initial azo-dye concentration at contact time = 120 min, azo dye concentrations = 5 mg/L, pH = 2, temperature = 23°C, zeolite NaX adsorbents dose = 0.3 g, and shaking rotary speed = 200 rpm.

0.3 g of zeolite NaX at pH 2 was impacted. The amount of azo dye removed rose from 58.34% to 87.56% after the speed of shaking was raised to 180 rpm with zeolite NaX, as shown in Fig. 5. With quicker shaking rates, there was a little decrease in the percentage of azo dye removal. The cause of this rise is that the relationship of the dyes with the surface of the adsorbent increased along with the shaking speed, which sped up the reaction between the anionic dye and positively charged adsorbents [46].

3.1.6. Optimum conditions

Using an adsorbent dosage of 0.3 g, 2 of pH, 5 mg/L of starting dye concentration, 180 rpm of shaking, and 120 min of contact time, the optimal values for zeolite NaX adsorbent were attained.

3.2. Adsorption isotherm

Fig. 6 shows the azo dye’s adsorption isotherms onto the adsorbent zeolite NaX. The optimal adsorbents dose was applied at 0.3 g of zeolite NaX during 120 min of stirring at 150 rpm, 23°C, and pH 2. Table 1 displays the correlation coefficient values for the Temkin (A , B , and R^2), Freundlich (k_f , n , and R^2), and Langmuir (q_e , b , and R^2) isotherms. Additionally, the Langmuir isotherm model, which fits dye adsorption on zeolite NaX the best and has a high R^2 value, is mentioned [47]. According to Table 1, all of the equilibrium parameter (R_L) values for the Langmuir isotherm model were the value between 0–1, indicating that the Langmuir isotherm is advantageous [48].

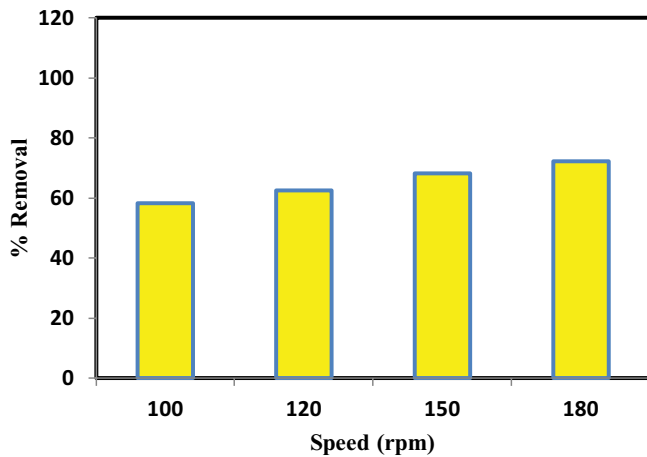


Fig. 5. Effect of shaking rotary speed on azo-dye removal at contact time = 120 min, azo dye concentrations = 5 mg/L, pH = 2, temperature = 23°C, and zeolite NaX adsorbents dose = 0.3 g.

3.3. Kinetics of adsorption

Adsorption assays were carried out to look at the kinetics of various dye concentrations at an optimal adsorbent dose at pH 2, 23°C, and 150 rpm agitation speeds over time intervals of 10–140 min. The values of the pseudo-first-order rate constant, k_1 , are reported in Table 2 and were derived from the linear plots of $\ln(q_e - q_t)$ vs. t (Fig. 7). The pseudo-second-order parameters (k_2 and q_e), which were determined

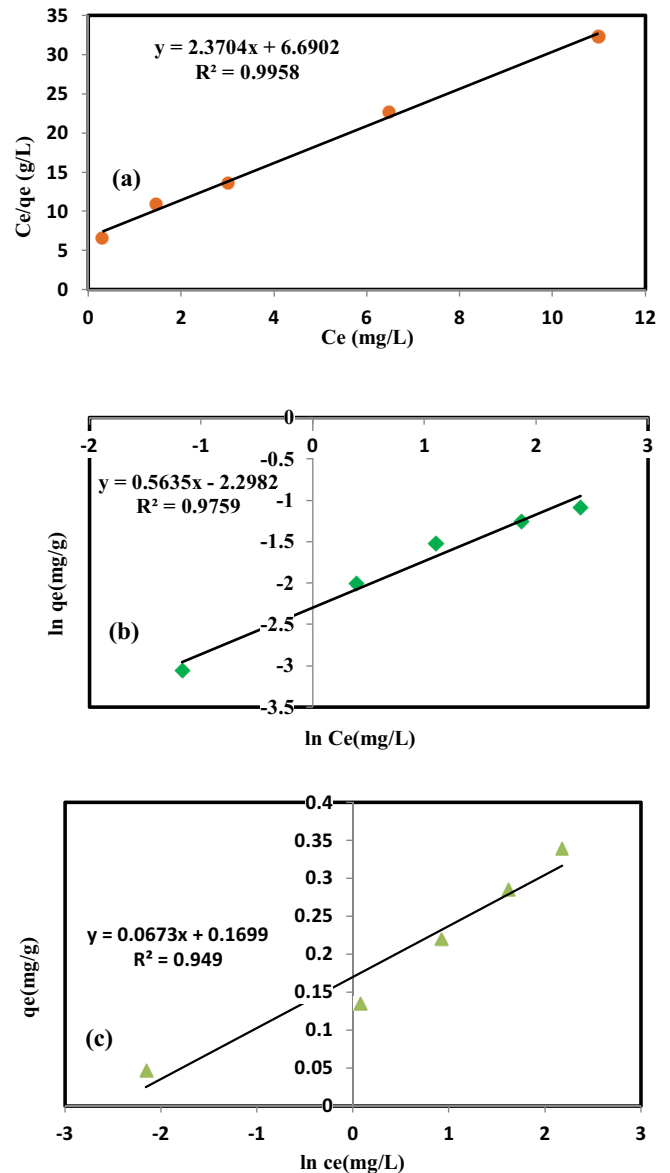


Fig. 6. (a) Langmuir, (b) Freundlich and (c) Temkin isotherms.

Table 1

Azo dye adsorption on zeolite NaX according to the Langmuir, Freundlich, and Temkin models

Adsorbents	Langmuir constants				Freundlich constants			Temkin constants		
	q_{max} (mg/g)	b (L/mg)	R^2	R_L	$1/n$	k_f	R^2	B	A (L/mg)	R^2
Zeolite NaX	0.42187	0.025	0.996	0.88	0.949	0.14612	0.459	0.067	12.484	0.949

Table 2

Constants of azo dye kinetics adsorption on zeolite NaX according to the pseudo-first-order, pseudo-second-order, and intraparticle diffusion model

Adsorbents	$q_{e,exp}$ (mg/g)	Pseudo-first-order constants			Pseudo-second-order constants			Intraparticle diffusion constants	
		$q_{e,cal}$ (mg/g)	k_1 (g/mg·min)	R^2	$q_{e,cal}$ (mg/g)	k_2 (g/mg·min)	R^2	k_{id} (mg/g·min ^{0.5})	R^2
Zeolite NaX	0.42187	0.437928	0.0042	0.989	0.170094	0.096061	0.9793	0.69	0.9463

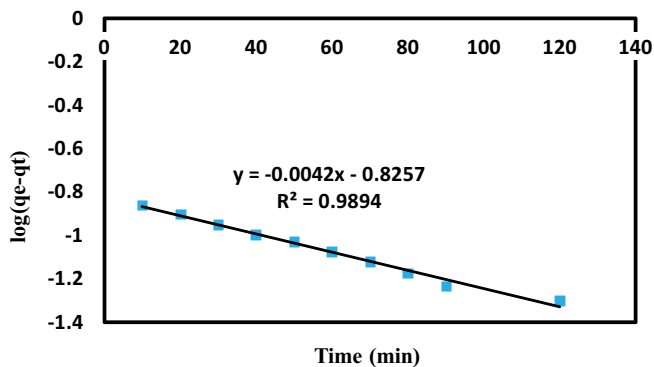


Fig. 7. Pseudo-first-order kinetic plot for adsorption of azo-dye over zeolite NaX.

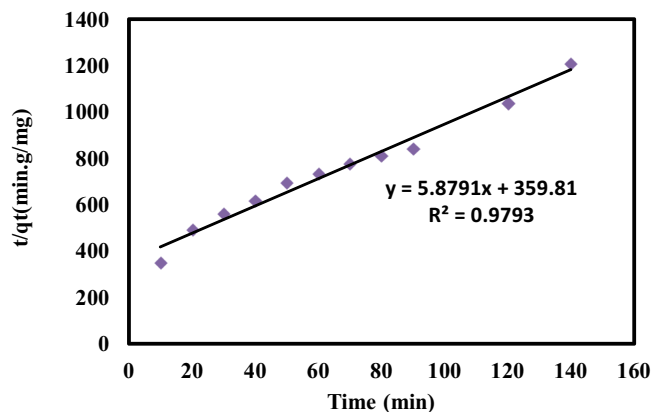


Fig. 8. Pseudo-second-order kinetic plot for adsorption of azo-dye over zeolite NaX.

using the slope and intercept from the plot of t/q_t against t (Fig. 8), were then assigned correlation coefficients in Table 2. The excellent linearity of the pseudo-first-order model was confirmed by the high R^2 values and graphs. The pseudo-first-order model was suitable to capture the adsorption kinetics of azo dye by zeolite NaX because the azo dye adsorption was a procedure with several stages that involved the adsorption onto the exterior layer and penetration into the inside of adsorbents [49].

In order to better understand the mechanism and rate-controlling mechanisms, the experimental findings were fitted to the intraparticle diffusion model in accordance with Eq. (9), as shown in Fig. 9. The larger slope of the dotted lines in this area is indicative of a higher gradient of concentration, as illustrated by Fig. 9, which illustrates dependency on external diffusion. This resulted from a decrease

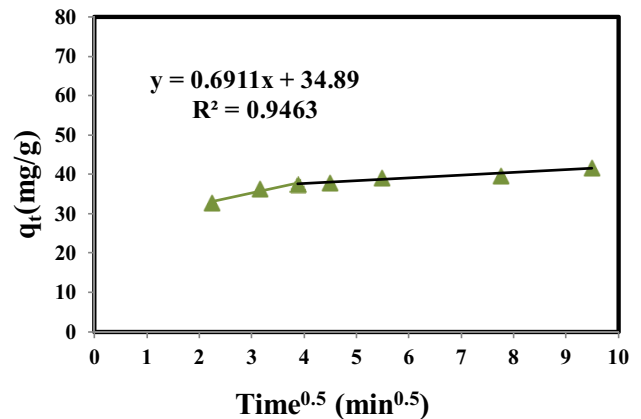


Fig. 9. Intraparticle diffusion model plot for adsorption of azo-dye over zeolite NaX.

in the gradient of azo-dye concentration and saturation of zeolite NaX external sites. Table 2 shows that k_{id} values is 0.6911 mg/g·min^{0.5} with determination coefficient $R^2 = 0.9463$.

4. Conclusion

According to the outcomes of the current experiment, when performed under the same operating conditions, using zeolite NaX was relatively efficient in removing azo dye from aqueous solutions. As azo dye removal continued, contact duration, the speed of shaking, and adsorbent dose all increased, whereas starting concentrations of azo dye and pH declined. At 5 mg/L, pH 2, and 180 rpm, the greatest quantity of azo dye was absorbed, which is comparable to a removal efficiency using zeolite NaX 72.34% at 0.3 g/100 mL of adsorbents. The optimal contact time for zeolite NaX was discovered after 120 min of exposure. The higher correlation coefficient of the adsorption data made it more compatible with the Langmuir model than with the Freundlich and Temkin models. The equilibrium parameter (R_L) values for the Langmuir isotherm model revealed that all R_L values were between 0 and 1, demonstrating the benefit of the Langmuir isotherm. This demonstrates that zeolite NaX is only marginally successful at removing the azo dye, which is uniformly dispersed in a monolayer coating on the adsorbent's exterior. The pseudo-first-order kinetic model was validated using adsorption studies.

Acknowledgments

The authors are grateful to the Department of Chemical Engineering at the University of Technology-Iraq, the Mustansiriyah University/College of Engineering/Materials

Engineering Department, Baghdad-Iraq, the Department of Chemical and Petroleum Industries Engineering, Al-Mustaqbal University, Babylon, Iraq.

Declarations

Ethics approval and consent to participate

Not applicable.

Competing interests

The authors declare that they have no competing interests.

Consent for publication

Not applicable.

Funding

Not Applicable

Availability of data and material

All relevant data and material are presented in the main paper.

References

- [1] A.M. Lotito, M. De Sanctis, C. Di Iaconi, G. Bergna, Textile wastewater treatment: aerobic granular sludge vs activated sludge systems, *Water Res.*, 54 (2014) 337–346.
- [2] P.A. Joshi, K.J. Mhatre, Microbial efficiency to degrade Carbol fuchsin and Malachite green dyes, *Adv. Appl. Sci. Res.*, 6 (2015) 85–88.
- [3] H. Yin, P. Qiu, Y. Qian, Z. Kong, X. Zheng, Z. Tang, H. Guo, Textile wastewater treatment for water reuse: a case study, *Processes*, 7 (2019) 34, doi: 10.3390/pr7010034.
- [4] V.S. Munagapati, D.-S. Kim, Adsorption of anionic azo dye Congo red from aqueous solution by cationic modified orange peel powder, *J. Mol. Liq.*, 220 (2016) 540–548.
- [5] Y.-H. Chiu, T.-F.M. Chang, C.-Y. Chen, M. Sone, Y.-J. Hsu, Mechanistic insights into photodegradation of organic dyes using heterostructure photocatalysts, *Catalysts*, 9 (2019) 430, doi: 10.3390/catal9050430.
- [6] O. Yesilada, E. Birhanli, H. Geckil, Bioremediation and Decolorization of Textile Dyes by White Rot Fungi and Laccase Enzymes, R. Prasad, Ed., *Mycoremediation and Environmental Sustainability*, Springer, Cham, 2018, pp. 121–153.
- [7] S.K. Al-Dawery, Enhanced dynamics characterization of photocatalytic decolorization of hazardous dye Tartrazine using titanium dioxide, *Desal. Water Treat.*, 57 (2016) 8851–8859.
- [8] S. Kim, C.M. Park, M. Jang, A. Son, N. Her, M. Yu, S. Snyder, D.-H. Kim, Y. Yoon, Aqueous removal of inorganic and organic contaminants by graphene-based nano-adsorbents: a review, *Chemosphere*, 212 (2018) 1104–1124.
- [9] J. Fu, T. Wen, Q. Wang, X.-W. Zhang, Q.-F. Zeng, S.-Q. An, H.-L. Zhu, Degradation of Active Brilliant Red X-3B by a microwave discharge electrodeless lamp in the presence of activated carbon, *Environ. Technol.*, 31 (2010) 771–779.
- [10] S.C. Santos, R.A. Boaventura, Treatment of a simulated textile wastewater in a sequencing batch reactor (SBR) with addition of a low-cost adsorbent, *J. Hazard. Mater.*, 291 (2015) 74–82.
- [11] P.I. Firmino, M.E. da Silva, F.J. Cervantes, A.B. dos Santos, Colour removal of dyes from synthetic and real textile wastewaters in one- and two-stage anaerobic systems, *Bioresour. Technol.*, 101 (2010) 7773–7779.
- [12] K.A. Amin, F.S. Al-Shehri, Toxicological and safety assessment of tartrazine as a synthetic food additive on health biomarkers: a review, *Afr. J. Biotechnol.*, 17 (2018) 139–149.
- [13] N.S. Ali, K.R. Kalash, A.N. Ahmed, T.M. Albayati, Performance of a solar photocatalysis reactor as pretreatment for wastewater via UV, UV/TiO₂, and UV/H₂O₂ to control membrane fouling, *Sci. Rep.*, 12 (2022) 16782, doi: 10.1038/s41598-022-20984-0.
- [14] S.M. Alardhi, J.M. Alrubaye, T.M. Albayati, Removal of Methyl Green Dye from Simulated Wastewater using Hollow Fiber Ultrafiltration Membrane, 2nd International Scientific Conference of Al-Ayen University (ISCAU-2020), IOP Conf. Ser.: Mater. Sci. Eng., 928 (2020) 052020, doi: 10.1088/1757-899X/928/5/052020.
- [15] S.T. Kadhum, G.Y. Alkindi, T.M. Albayati, Determination of chemical oxygen demand for phenolic compounds from oil refinery wastewater implementing different methods, *Desal. Water Treat.*, 231 (2021) 44–53.
- [16] A.T. Khadim, T.M. Albayati, N.M. Cata Saady, Removal of sulfur compounds from real diesel fuel employing the encapsulated mesoporous material adsorbent Co/MCM-41 in a fixed-bed column, *Microporous Mesoporous Mater.*, 341 (2022) 112020, doi: 10.1016/j.micromeso.2022.112020.
- [17] N.M. Jabbar, S.M. Alardhi, A.K. Mohammed, I.K. Salih, T.M. Albayati, Challenges in the implementation of bioremediation processes in petroleum-contaminated soils: a review, *Environ. Nanotechnol. Monit. Manage.*, 18 (2022) 100694, doi: 10.1016/j.enmm.2022.100694.
- [18] H.J. Al-Jaaf, N.S. Ali, S.M. Alardhi, T.M. Albayati, Implementing eggplant peels as an efficient bio-adsorbent for treatment of oily domestic wastewater, *Desal. Water Treat.*, 245 (2022) 226–237.
- [19] N.S. Ali, N.M. Jabbar, S.M. Alardhi, H.Sh. Majdi, T.M. Albayati, Adsorption of methyl violet dye onto a prepared bio-adsorbent from date seeds: isotherm, kinetics, and thermodynamic studies, *Heliyon*, 8 (2022) e10276, doi: 10.1016/j.heliyon.2022.e10276.
- [20] N.S. Ali, H.N. Harharah, I.K. Salih, N.M. Cata Saady, S. Zendejboudi, T.M. Albayati, Applying MCM-48 mesoporous material, equilibrium, isotherm, and mechanism for the effective adsorption of 4-nitroaniline from wastewater, *Sci. Rep.*, 13 (2023) 9837, doi: 10.1038/s41598-023-37090-4.
- [21] M.L.G. Vieira, M.S. Martinez, G.B. Santos, G.L. Dotto, L.A. Pinto, Azo dyes adsorption in fixed bed column packed with different deacetylation degrees chitosan coated glass beads, *J. Environ. Chem. Eng.*, 6 (2018) 3233–3241.
- [22] D. Akolekar, A. Chaffee, R.F. Howe, The transformation of kaolin to low-silica X zeolite, *Zeolites*, 19 (1997) 359–365.
- [23] M. Murat, A. Amokrane, J.P. Bastide, L. Montanaro, Synthesis of zeolites from thermally activated kaolinite. Some observations on nucleation and growth, *Clay Miner.*, 27 (1992) 119–130.
- [24] J.M. Salazar, S. Lectez, C. Gauvin, M. Macaud, J.P. Bellat, G. Weber, I. Bezverkhy, J.M. Simon, Adsorption of hydrogen isotopes in the zeolite NaX: experiments and simulations, *Int. J. Hydrogen Energy*, 42 (2017) 13099–13110.
- [25] D. Ramimoghdam, S. Bagheri, S.B. Abd Hamid, Progress in electrochemical synthesis of magnetic iron oxide nanoparticles, *J. Magn. Magn. Mater.*, 368 (2014) 207–229.
- [26] Y. Liu, L. Liu, J. Shan, J. Zhang, Electrodeposition of palladium and reduced graphene oxide nanocomposites on foam-nickel electrode for electrocatalytic hydrodechlorination of 4-chlorophenol, *J. Hazard. Mater.*, 290 (2015) 1–8.
- [27] W.A. Muslim, S.K. Al-Nasri, T.M. Albayati, Evaluation of bentonite, attapulgite, and kaolinite as eco-friendly adsorbents in the treatment of real radioactive wastewater containing Cs-137, *Prog. Nucl. Energy*, 162 (2023) 104730, doi: 10.1016/j.pnucene.2023.104730.
- [28] N.S. Abbood, N.S. Ali, E.H. Khader, H.Sh. Majdi, T.M. Albayati, N.M. Cata Saady, Photocatalytic degradation of cefotaxime pharmaceutical compounds onto a modified nanocatalyst, *Res. Chem. Intermed.*, 49 (2023) 43–56.
- [29] W.A. Muslim, T.M. Albayati, S.K. Al-Nasri, Decontamination of actual radioactive wastewater containing ¹³⁷Cs using

- bentonite as a natural adsorbent: equilibrium, kinetics, and thermodynamic studies, *Sci. Rep.*, 12 (2022) 13837, doi: 10.1038/s41598-022-18202-y.
- [30] F.K. Mostafapour, M. Yilmaz, A.H. Mahvi, A. Younesi, F. Ganji, D. Balarak, Adsorptive removal of tetracycline from aqueous solution by surfactant-modified zeolite: equilibrium, kinetics and thermodynamics, *Desal. Water Treat.*, 247 (2022) 216–228.
- [31] M. Vadi, A.O. Mansoorabad, M. Mohammadi, N. Rostami, Investigation of Langmuir, Freundlich and Temkin adsorption isotherm of tramadol by multi-wall carbon nanotube, *Asian J. Chem.*, 25 (2013) 5467–5469.
- [32] H. Yuh-Shan, Citation review of Lagergren kinetic rate equation on adsorption reactions, *Scientometrics*, 59 (2004) 171–177.
- [33] D. Balarak, M. Baniyasi, S. Lee, M.J. Shim, Ciprofloxacin adsorption onto *Azolla filiculoides* activated carbon from aqueous solutions, *Desal. Water Treat.*, 218 (2021) 444–453.
- [34] D. Balarak, A.H. Mahvi, M.J. Shim, S. Lee, Adsorption of ciprofloxacin from aqueous solution onto synthesized NiO: isotherm, kinetic and thermodynamic studies, *Desal. Water Treat.*, 212 (2021) 390–400.
- [35] Y.S. Ho, Review of second-order models for adsorption systems, *J. Hazard. Mater.*, 136 (2006) 681–689.
- [36] N. Kannan, T. Veemaraj, Removal of lead(II) ions by adsorption onto bamboo dust and commercial activated carbons-a comparative study, *E-J. Chem.*, 6 (2009) 247–256.
- [37] N. Kannan, M. Meenakshisundaram, Adsorption of Congo red on various activated carbons. A comparative study, *Water Air Soil Pollut.*, 138 (2002) 289–305.
- [38] N. Kannan, A. Xavier, New composite mixed adsorbents for the removal of acetic acid by adsorption from aqueous solutions - a comparative study, *Toxicol. Environ. Chem.*, 79 (2001) 95–107.
- [39] S. Banerjee, M.C. Chattopadhyaya, Adsorption characteristics for the removal of a toxic dye, tartrazine from aqueous solutions by a low-cost agricultural by-product, *Arabian J. Chem.*, 10 (2017) S1629–S1638.
- [40] H.O. Chukwuemeka-Okorie, F.K. Ekuma, K.G. Akpomie, J.C. Nnaji, A.G. Okerefor, Adsorption of tartrazine and sunset yellow anionic dyes onto activated carbon derived from cassava sieve biomass, *Appl. Water Sci.*, 11 (2021) 1–8.
- [41] U. Filipkowska, T. Jozwiak, J. Rodziewicz, J. Kuciejewska, Application of maize silage as a biosorbent for the removal of dyes from aqueous solutions, *Rocznik Ochrona Srodowiska*, 15 (2013) 2324–2338.
- [42] A. Saad, I. Bakas, J.Y. Piquemal, S. Nowak, M. Abderrabba, M.M. Chehimi, Mesoporous silica/polyacrylamide composite: preparation by UV-graft photopolymerization, characterization and use as Hg(II) adsorbent, *Appl. Surf. Sci.*, 367 (2016) 181–189.
- [43] S. Yadav, A. Asthana, R. Chakraborty, B. Jain, A.K. Singh, S.A.C. Carabineiro, Md.A.B.H. Susan, Cationic dye removal using novel magnetic/activated charcoal/ β -cyclodextrin/alginate polymer nanocomposite, *Nanomaterials*, 10 (2020) 170, doi: 10.3390/nano10010170.
- [44] A.E. Mahdi, N.S. Ali, H.Sh. Majdi, T.M. Albayati, M.A. Abdulrahman, D.J. Jasim, K.R. Kalash, I.K. Salih, Effective adsorption of 2-nitroaniline from wastewater applying mesoporous material MCM-48: equilibrium, isotherm, and mechanism investigation, *Desal. Water Treat.*, (2023) 1–10, doi: 10.5004/dwt.2023.29741.
- [45] S. Chawla, H. Uppal, M. Yadav, N. Bahadur, N. Singh, Zinc peroxide nanomaterial as an adsorbent for removal of Congo red dye from wastewater, *Ecotoxicol. Environ. Saf.*, 135 (2017) 68–74.
- [46] T. Józwiak, U. Filipkowska, S. Brym, L. Kopeć, Use of aminated hulls of sunflower seeds for the removal of anionic dyes from aqueous solutions, *Int. J. Environ. Sci. Technol.*, 17 (2020) 1211–1224.
- [47] H. Ouassif, E.M. Moujahid, R. Lahkale, R. Sadik, F.Z. Bouragba, E.M. Sabbar, M. Diouri, Zinc-aluminum layered double hydroxide: high efficient removal by adsorption of tartrazine dye from aqueous solution, *Surf. Interfaces*, 18 (2020) 100401, doi: 10.1016/j.surfin.2019.100401.
- [48] Y.A. Abd Al-Khodir, T.M. Albayati, Real heavy crude oil desulfurization onto nanoporous activated carbon implementing batch adsorption process: equilibrium, kinetics, and thermodynamic studies, *Chem. Afr.*, 6 (2023) 747–756.
- [49] T.M. Albayati, A.A. Sabri, D.B. Abed, Adsorption of binary and multi heavy metals ions from aqueous solution by amine functionalized SBA-15 mesoporous adsorbent in a batch system, *Desal. Water Treat.*, 151 (2019) 315–321.